Journal of Fluorine Chemistry 132 (2011) 19–26

Contents lists available at ScienceDirect

Journal of Fluorine Chemistry

journal homepage: www.elsevier.com/locate/fluor

Effect of acid on morphology of calcite during acid enhanced defluoridation

Suresh K. Nath, Shreemoyee Bordoloi, Robin K. Dutta *

Department of Chemical Sciences, Tezpur University, Napaam, Tezpur 784028, India

ARTICLE INFO

Article history:
Received 17 August 2010
Received in revised form 27 October 2010
Accepted 28 October 2010
Available online 3 November 2010

Keywords:
Defluoridation
Limestone
Calcite
Acetic acid
Citric acid

ABSTRACT

Fluoride removal from water by lime materials is a promising defluoridation process. Acid enhanced limestone defluoridation (AELD) technique involves precipitation of CaF_2 as well as adsorption of fluoride on the surface of limestone which is capable of reducing fluoride concentration to below the WHO guideline value of 1.5 mg/L. Acids such as acetic acid and citric acid are added to the fluoride water before filtration through limestone column to enhance the Ca^{2+} activity in solution for precipitation of fluoride as CaF_2. This paper describes the effects of these acids on the quality of the limestone during the AELD process, which has been studied to evaluate the reusability of the limestone. The reaction products that formed during the AELD process have also been analyzed. The detail study of the morphology of the limestone before and after use have been done using various analytical techniques, *viz.*, X-ray diffraction, infrared spectroscopy, thermogravimetric analysis and scanning electron microscopy combined with energy dispersive X-ray spectroscopy. The study reveals that the limestone degrades to some extent in the process due to dissolution of calcium carbonate by the acids and adsorption of fluoride by the limestone. While appreciable quantity of the citrate salt of calcium was formed in the column, the acetate salt mostly remained dissolved in the water. Since mainly the surface of the limestone particles take part in the reaction, the limestone particles can be reused for the defluoridation process after cleaning the outer surface. The limestone after use remains also suitable as raw material for cement.

1. Introduction

Consumption of fluoride higher than the prescribed level for a prolonged period leads to fluorosis in both human and animals. Excessive amount of fluoride present in water is responsible for multidimensional health disorders, like mottling of teeth, softening of bones and ossification of tendons and ligaments [1–3]. The maximum permissible contaminant level of fluoride in drinking water is 1.5 mg/L in Indian standard [4] which is the same as the WHO guideline value [5].

The principles that are used for fluoride removal are based on adsorption [6–9], precipitation–coagulation [10,11], ion-exchange [12], membrane separation process [13,14], electrolytic defluoridation [15], electrodialysis [16–19], etc. Some recently used adsorbent for fluoride are laterite [20], waste residue from alum manufacturing plant [21], activated carbon prepared from Morringa Indica bark [22], carboxymethylated starch-based hydrogels loaded with Fe^{2+} [23], alum-impregnated activated alumina [24], etc. However, due to high cost, low efficiency or production of huge amount of sludge containing fluoride they do not find practical field utility. Calcium metal containing compounds have constantly been used in many fluoride affected areas to remove fluoride from water due to the potentiality of this metal for this process [25–27]. Calcium hydroxide [$Ca(OH)_2$] is used for separation of fluoride from drinking water. Calcium chloride [$CaCl_2$] and calcium sulphate [$CaSO_4$] are used in treatment of industrial waste water containing fluoride [28]. The study of the reaction between limestone and fluoridated water has continuously been of great importance due to the fluoride uptake capacity of limestone. It has been used for precipitation of fluoride from industrial wastewater as well as for purification of groundwater. Limestone can not only precipitate fluoride as calcium fluoride, it also adsorbs fluoride ions [25]. The transition of calcium carbonate into fluorite is a slow process and fluorite grains formed are very strong [29]. After reaction is carried out by stirring, fluorites exist as stable suspension, which is difficult to filter and therefore, it is better to carry out such reaction by passing fluoride solution through a calcite bed or a column reactor [29]. Limestone treatment of fluoride contaminated water has been reported to reduce fluoride level below 4 mg/L [30]. In situ generation of Ca^{2+} ions in crushed limestone column by passing CO_2 through the limestone column can reduce the fluoride level below 2 mg/L [11]. Use of HCl with calcite is also useful for removal of fluoride from industrial wastewater [27]. When initial concentration of fluoride

* Corresponding author. Tel.: +91 3712 267007/8/9x5055; fax: +91 3712 267005/6.
E-mail addresses: suresh@tezu.ernet.in (S.K. Nath), sh_momy@tezu.ernet.in (S. Bordoloi), robind@tezu.ernet.in (R.K. Dutta).

0022-1139/$ – see front matter © 2010 Elsevier B.V. All rights reserved.
doi:10.1016/j.jfluchem.2010.10.007

is large, e.g. in wastewater, it is easier to precipitate fluoride as CaF_2 since it attains supersaturation level easily, however when fluoride strength is low, it is difficult to precipitate [31]. So it is a challenge to decrease the fluoride from lower strength, i.e., from 10 to 20 mg/L to drinking water level by precipitation method without the need of pH correction. To meet this challenge we have done the experiment using edible acids and obtained promising results [32,33]. Use of the edible acids, viz., acetic acid (AA) and citric acid (CA) for the acid enhanced limestone defluoridation has been found to reduce the fluoride to below 1.5 mg/L which has been considered as a potential technique for rural groundwater defluoridation applications [33]. An investigation of the mechanism of fluoride removal when citric acid and acetic acid were used revealed the removal to be a combined result of precipitation of calcium fluoride by the calcium ion generated by dissolution of calcium carbonate and adsorption of fluoride on limestone surface [33]. However the extent of damage done to the limestone in the process has not been ascertained analytically, which is important for reuse of the limestone for further fluoride removal or disposal as a raw material for cement manufacture.

There are three different forms of calcium carbonate (limestone) occurring in nature: the Trigonal Hexagonal Scalenohedral crystal known as *calcite*, orthorhombic form *aragonite* and hexagonal dihexagonal dipyramidal form *vaterite*. Calcite is the most abundant form and is widely distributed in the Earth's crust followed by aragonite and vaterite. There is another comparatively rare mineral dolomite which is a mixture of $CaCO_3$ and $MgCO_3$ [34]. Calcite is a sedimentary rock and it is the most important raw material for the manufacture of cement.

Knowledge of morphological and chemical changes of the limestone during the process is quite relevant with respect to upscaling the fluoride removal technique and reuse of the used limestone. Glover and Sippel have studied the reaction between calcite and 1–50% HF solution which results in pseudomorphic replacement by epitaxial growth of the (1 1 0) of fluorite in the (1 0 1 1) plane of calcite [35]. Simonson has studied the removal of fluoride by limestone treatment and used some kinetic as well as mathematical model for the removal analysis [36]. The studies of Simonson, Reardon et al., Turner et al. and Yang et al. on limestone were well carried out, but the waste disposal was not addressed [11,25,27,36]. In our previous paper, though we had reported a detail study of the AELD method with AA and CA, only a preliminary study was reported on the quality of the limestone after use [33]. In the present work, the quality of the used limestone and the byproducts formed have been characterized using several analytical tools to see the whether the limestone can be reused or whether any other toxic chemicals are produced in the AELD process.

X-ray diffraction study is one of the most important techniques for analyzing solid samples like calcite. The reactions of calcite with fluoridated and with carbonated fluoride water have earlier been studied with different analytical techniques like X-ray diffraction (XRD), Fourier transform infrared spectroscopy (FTIR), Raman, X-ray photoelectron spectroscopy (XPS) or electron spectroscopy for chemical analysis (ESCA), atomic force microscopy (AFM), etc., to establish the different reaction products and intermediates produced during the course of the reaction [25,29]. Scanning electron microscopy combined with energy dispersive X-ray spectroscopy (SEM-EDX) and optical microscopy has also been used earlier in order to examine the morphological effects of different reactants and circumstances on lime material [37,38]. The morphological changes to the crushed limestone after use in fixed bed for fluoride removal from fluoridated water acidified with citric acid or acetic acid have not been studied in detail in our previous report [33]. In this present study 10 mg/L fluoride containing water in presence of two edible acids has been treated with crushed crude limestone column fixed bed for a contact time of 12 h and the degradation of limestone as well as the changes in the limestone surface has been studied by using X-ray diffraction, infra-red spectroscopy, thermal techniques and scanning electron microscopy. Some X-ray photoelectron spectra results of our previous study of the limestone before and after use have also been discussed in this study as complementary.

Two particle sizes of limestone, *viz.*, 2–3 mm and 3–4 mm, were used initially for the fluoride removal experiments [33]. As the 2–3 mm size gave better removal due to larger surface area than 3–4 size, the present study was restricted to the 2–3 mm particle size.

2. Results and discussion

2.1. Defluoridation by limestone column in presence of the acids

In the fluoride removal experiment conducted using the two acids it has been found that, in the presence of the acids, limestone can remove fluoride from 10–20 mg/L to below 1.5 mg/L [33]. Both the acids showed almost similar fluoride removal ability. In the experiment of fluoride removal using limestone in presence of CA, we have found a powdery precipitate in the lower part of the column. When the reaction was carried out in presence of AA, no such powdered material was found on the limestone surface. This is probably due to the high solubility of the calcium acetate salt which remained in the treated water in soluble form. However when the water was filtered through Whatman 42 filter paper some precipitate has been observed on the side of the filter paper. The composition of these materials also have been analyzed along with the study of the changes in the used limestone by different analytical techniques, *viz.*, powder X-ray, FTIR, DSC, TGA and SEM-EDX has been used. The results have been compared with standard data as described below.

The same crushed limestone column was charged with the acidified fluoride containing water every day and discharged in two or three parts after 6, 12 and 24 h of residence time. The AELD process with AA and CA could reduce the fluoride concentration from 10 mg/L to below 2 mg/L up to 12th repeated use of the of the same crushed limestone column. The limestone chips were then washed with fluoride free water to remove the precipitates formed on the surface of the limestone and dried in air. The regenerated limestone chips were found only slightly less effective than the fresh ones. Reuse of the regenerated limestone chips showed F^- removal to below 2 mg/L up to further 10th repeated use of the same crushed limestone column. The observed regeneration of the activity of the limestone chips just by washing indicates that only the surface the limestone is degraded during the AELD process forming calcium fluoride and calcium acetate or calcium citrate. Though adsorption takes place [25,33] along with the precipitation, the deactivation of the limestone due to the adsorption is minimal. Renewal of the limestone surface by dissolution during reaction with the acids also minimizes the deactivation of the limestone caused by saturation with adsorbed fluoride [25].

2.2. X-ray diffraction analysis

The X-ray diffraction patterns of the limestone before and after reaction with different acid containing fluoridated water have been shown in Fig. 1. It can be seen from Fig. 1A that the intensity and the distance between crystal planes of diffraction peaks are in good agreement with the standard spectrum of the crystalline calcite polymorph of calcium carbonate. The 2θ values of the XRD spectrum which are 23°, 29.5° (strong), 36.12°, 39.5°, 43.5°, 47.5° and 48.5°; correspond to the calcite polymorph of calcium carbonate [*d* spacings (Å): 3.86 (1 0 2), 3.02 (1 0 4), 2.48 (1 1 0),

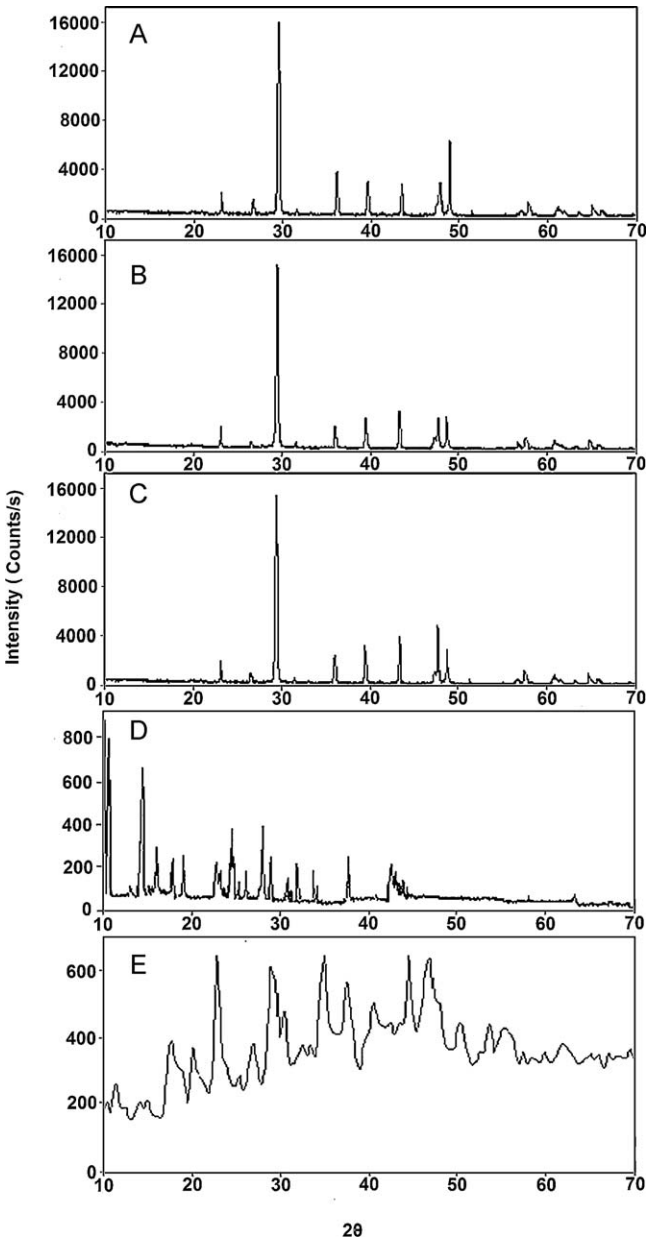

Fig. 1. The X-ray diffraction spectrum of (A) crude limestone, (B) limestone after use with acetic acid, (C) limestone after use with citric acid, (D) precipitate obtained with AA and (E) precipitate obtained with CA.

2.27 (1 1 3), 2.07 (2 0 2), 1.91 (1 0 8) and 1.87 (1 1 6), respectively] [39,40].

The X-ray diffraction pattern of the limestone after use in the reaction shows some difference with that recorded before use (Fig. 1B and C). The relative intensities of the peaks at 36.12°, 39.5°, 43.5° reversed after use of the limestone indicating relative damage to the respective planes decreasing in the order (1 1 0) > (1 1 3) > (2 0 2). The extent of the changes in the relative intensities is more in the case of the limestone used with AA than that used with CA with equal exposure to the acidic fluoride solutions. This indicates greater morphological effect of AA than that of CA on the limestone. On the other hand, the relative intensities of the peaks at 47.5°, and 48.5° also reversed after use of the limestone whereas the peak at 47.5° corresponding to plane (1 0 8) is expected to be diminished more that of the peak at 48.5° which corresponds to the plane (1 1 6). The increase in the relative peak intensity at 47.5° can be attributed to diffraction from the plane (2 0 2) of fluorite (CaF_2) which gives rise to a strong intensity [29,41]. This indicates formation of fluorite on the limestone surface due to the reaction of free Ca^{2+} produced by dissolution of limestone in presence of acid, adsorption of fluoride on limestone or due to penetration by fluoride slightly into the limestone. The above variations in the X-ray diffraction pattern however do not indicate very significant changes in the limestone after use in for the defluoridation.

The X-ray diffraction pattern of the powdery substance obtained during defluoridation in the presence of CA is as shown in spectra E in Fig. 1, which is similar to the X-ray diffraction spectra of laboratory grade calcium citrate. This indicates the powdered compound produced on the surface of the limestone to be calcium citrate. Similarly, the XRD spectrum of the precipitate obtained when AA was used (spectra D in Fig. 1) resembles with the reported X-ray spectrum of calcium acetate crystals [42]. The observed formation of the precipitate of calcium citrate on the limestone surface may block further reaction of CA or F^- with the limestone. Thus, the observed less significant morphological change of the limestone by CA than AA may be attributed to inhibition of limestone degradation by precipitates of calcium citrate.

2.3. IR studies

The IR spectrum of carbonate minerals show three prominent absorption bands in the regions ν_3 = 1450–1420, ν_2 = 890–870 and ν_4 = 720–700 cm^{-1}. The IR spectra of different limestone samples before and after treatment of the acidified fluoride containing water along with the powdered precipitate formed with CA and AA are shown in Fig. 2 and the characteristic wavenumbers are presented in Table 1. The main peak positions of the present crude limestone sample have been estimated at 1429, 875 and 711 cm^{-1}, respectively; which are consistent with that of reference $CaCO_3$ (Fig. 2) [34]. An observed broadening of the ν_3 peak may be due to the crystal field effects [43]. A comparison of the IR spectrum of the crude limestone with the calcite standard infrared spectrum indicates the crystal structure of the limestone sample to be high purity calcite. The IR spectra of the used limestone samples after separation from the precipitate formed on the surface are almost identical with that of the limestone before use. This indicates absence of a significant adsorption or penetration by citrate or acetate ions into the limestone crystal.

It can be observed from the IR data that O–H stretching frequency is apparent in all the spectra of used limestone ranging from 3350 to 3450 cm^{-1} (Table 1). For used limestone, water may penetrate to the core of the particles and even after drying some portion of moisture remained in the used limestone. In the precipitates, the presence of O–H bond stretching may be due to hygroscopic nature of the substances. Two small bands near 3000 cm^{-1} can be seen in the spectra of calcium acetate and calcium citrate, which is due to C–H stretching. The band near 1430 cm^{-1} in parent limestone remains at the same position in the used limestone which is characteristic position of carbonate minerals. After reaction with acetic acid and citric acid containing fluoride water, limestone forms corresponding salts of carboxylic acids, which is indicated by the two bands at 1609.89 and 1615.50 cm^{-1} for the antisymmetric stretching of O–C–O bonds and the two bands at 1446.89 and 1434.90 cm^{-1} for the symmetric stretching of the carboxylate groups of calcium acetate and calcium citrate, respectively [44,45]. The higher observed frequencies compared to that of the free COO^- indicate the ionic character of metal–COO^- coordinate bond which is also theoretically proved earlier [45]. In the spectra of carboxylate salts the carbonyl stretching frequency is lowered from the value found for the parent carboxylic acid because the O–C–O bond

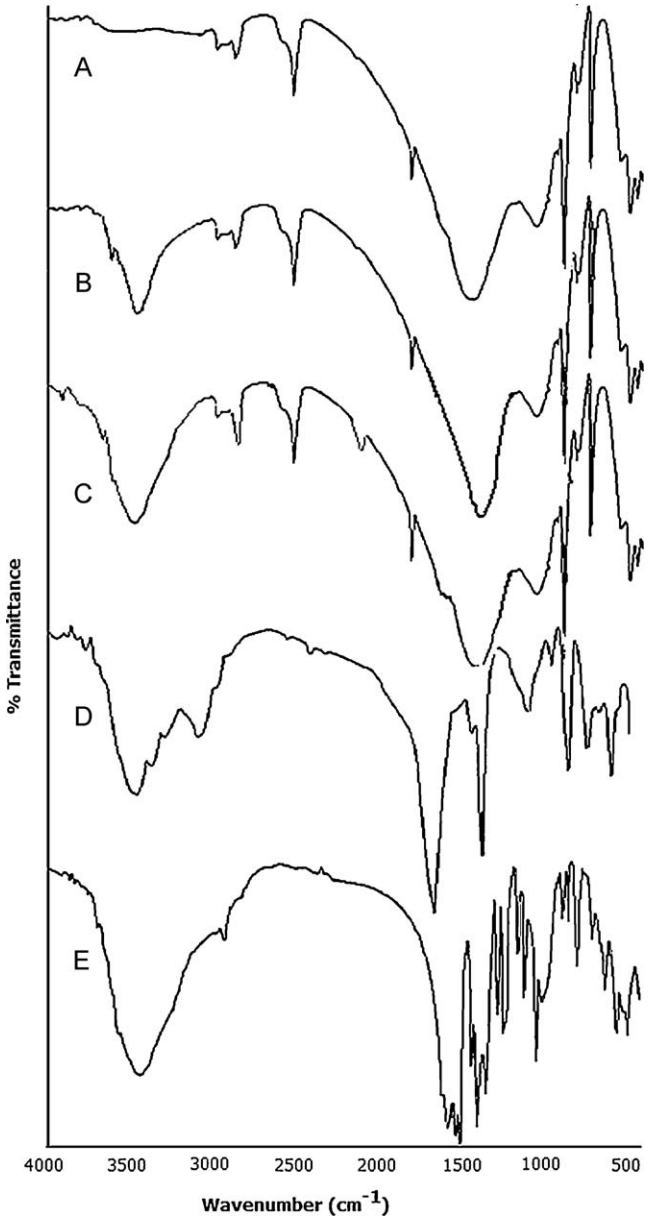

Fig. 2. IR spectra of (A) crude limestone, (B) limestone after use with acetic acid, (C) limestone after use with citric acid, (D) precipitate obtained with AA and (E) precipitate obtained with CA.

possesses more single-bond character due to resonance [46]. The IR frequencies of the precipitate obtained with citric acid and acetic acid have been found to be similar to the IR of laboratory grade calcium citrate and reported IR of calcium acetate [42] indicating the precipitates to be calcium citrate and calcium acetate, respectively.

2.4. TGA analysis

TGA analysis of the limestone before and after use with AA and CA, and of the precipitates obtained with AA and CA has been carried out in the temperature range of 0–700 °C and the mass loss *vs.* temp curves have been presented in Fig. 3. Calcium carbonate normally starts to decompose above 800 °C [47]. When a material is near to 100% pure it melts sharply. Presence of impurity lowers the final melting temperature and the melting usually occurs over a wider range [48]. The TGA curve of the present crude limestone before use (Fig. 3A) shows a slow decomposition of the material from 472 °C onwards, which may be due to the presence of some impurities. From 600 to 700 °C there is a relatively sharper mass loss, which indicates the starting of degradation of $CaCO_3$. The TGA obtained for limestone after use with AA (Fig. 3B) and CA (Fig. 3C) are identical with that obtained before use indicating absence of any significant degradation of the limestone during the defluoridation process.

In the TGA curve of the precipitate obtained after limestone treatment using AA (Fig. 3D), three significant mass losses have been observed at 120, 402 and 596 °C. The mass loss at 120 °C can be attributed to evaporation of water molecule followed by loss of carbon dioxide at 402 °C and finally loss of CO_2 to form stable calcium oxide at 596 °C [42]. Thus the curve corresponds to calcium acetate formed by combination of acetate ion and calcium ions dissolved from limestone. In the TGA curve of the precipitate obtained after limestone treatment using CA (Fig. 2E) two significant mass losses have been observed at 128 and 450 °C. The endothermic peak at 128 °C in Fig. 2E is due to the removal of water molecule present within the calcium citrate powder. The sharp mass loss at 450 °C may be due to the decomposition of calcium citrate [49]. The decomposition pattern also resembles with the TGA curve of pure calcium citrate indicating the precipitate to be calcium citrate.

2.5. DSC studies

DSC of different limestone before and after reaction has been studied at a heating rate of 10 °C min^{-1} in N_2 atmosphere using Al_2O_3 as reference. The results are shown in Fig. 4. In the reaction of limestone with fluoridated water containing acetic and citric acid, a part of $CaCO_3$ has been converted to respective calcium carboxylates which contains thermally less stable water of crystallization. In all DSC curves, endothermic peaks below 200 °C may be due to removal of water molecules. The exothermic peak in the range of 400–500 °C indicates the decomposition of carboxylates as well as remaining carbonates [49]. Thus the DSC curves also support the formation of calcium carboxylates.

Table 1
Characteristic wavenumbers (cm^{-1}) of the limestone before use and after use along with the precipitates formed after reaction of the limestone with AA and CA.

Crude limestone	Limestone after use with AA	Limestone after use with CA	Precipitate formed with AA	Precipitate formed with CA
	3425.71 (O–H stretching)	3431.13 (O–H stretching)	3378.27 (O–H stretching)	3447.30 (O–H stretching)
1429.23 (asymmetric stretching of O–C–O)	1428.27 (asymmetric stretching of O–C–O)	1428.10 (asymmetric stretching of O–C–O)	1609.89 (asymmetric stretching of O–C–O)	1615.50 (asymmetric stretching of O–C–O)
1032.65 (symmetric stretching of O–C–O)	1027.35 (symmetric stretching of O–C–O)	1029.21 (symmetric stretching of O–C–O)	1446.89 (symmetric stretching of O–C–O)	1434.90 (symmetric stretching of O–C–O)
			949.69 (stretching of C–C)	1078.59 (out of plane stretching of C–H)
857.44 (asymmetric CO_3 deformation)	873.83 (asymmetric CO_3 deformation)	874.20 (asymmetric CO_3 deformation)	671.09 (symmetric twisting and rocking of the O–C–O)	839.74 (bending out of plane C–H)
711.94 (symmetric CO_3 deformation)	708.22 (symmetric CO_3 deformation)	708.76 (symmetric CO_3 deformation)	620.50 (out-of-plane stretching vibrations of the O–C–O)	605.56 (out-of-plane stretching vibrations of the O–C–O)

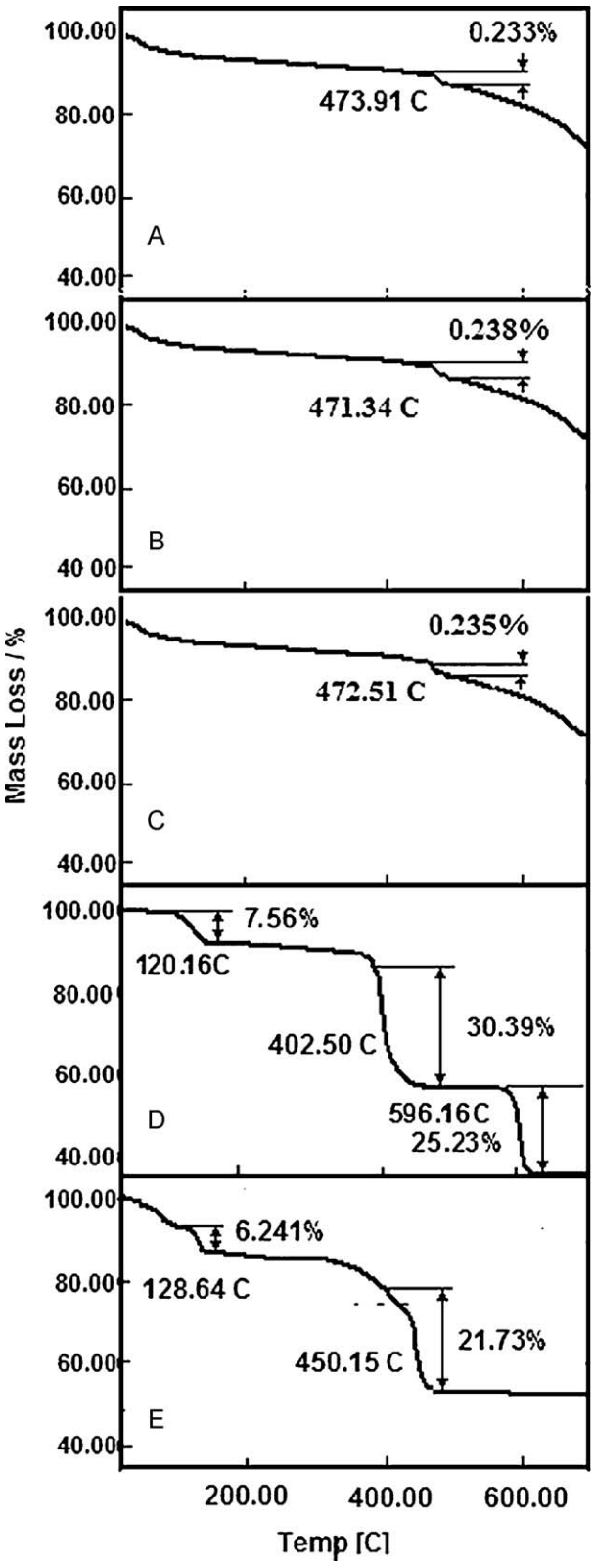

Fig. 3. Thermogravimetric analysis of limestone samples before and after treatment (A) crude limestone, (B) limestone after use with acetic acid, (C) limestone after use with citric acid, (D) precipitate obtained with AA and (E) precipitate obtained with CA.

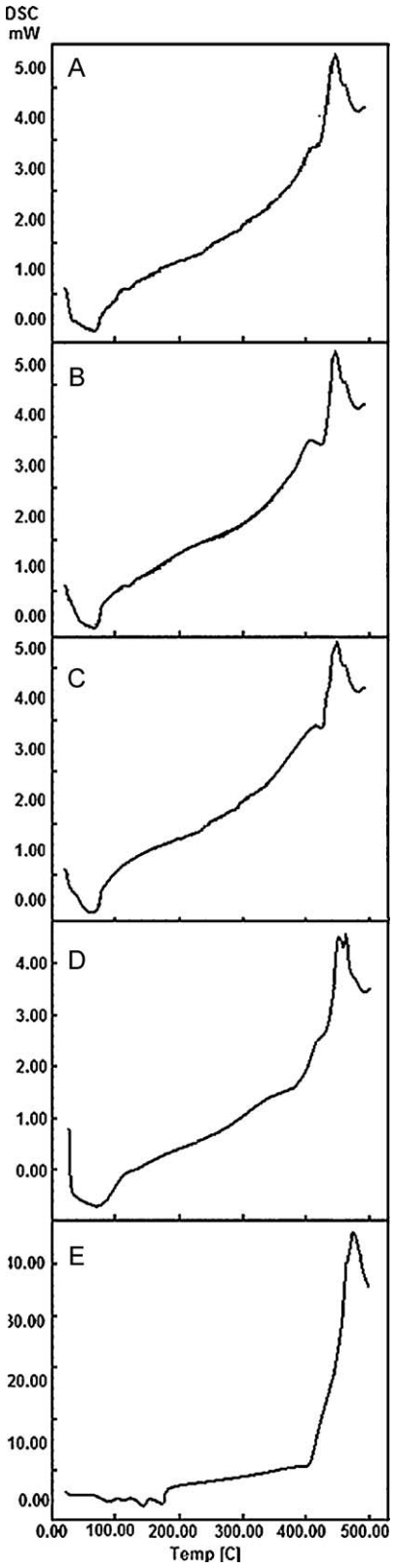

Fig. 4. DSC curves of the limestone samples before and after use (A) crude limestone, (B) limestone after use with acetic acid, (C) limestone after use with citric acid, (D) precipitate obtained with AA and (E) precipitate obtained with CA.

2.6. SEM-EDX study

SEM micrographs of the limestone samples before and after use with AA and CA containing fluoridated water have been taken to see the surface morphology change. To quantify the elements present in the limestone surface energy dispersive X-ray spectroscopy or EDX has been used along with SEM analysis. The EDX clearly shows the presence of fluoride in the sample after use (Fig. 5B and C). The weight and atomic percentage of the elements have been shown in Table 2. From these values one

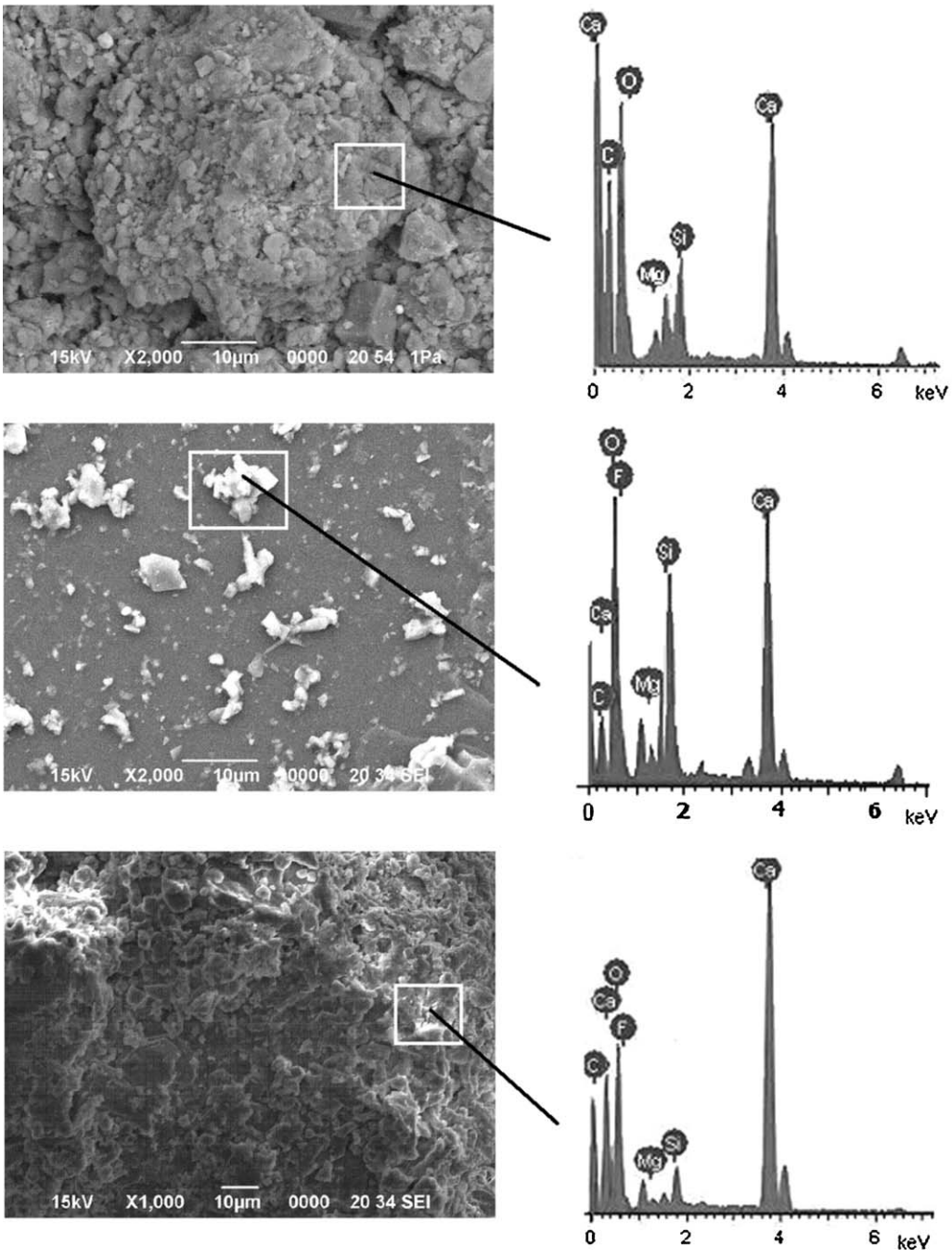

Fig. 5. SEM and EDX of limestone: (A) before use, (B) after use with AA and (C) after use with CA.

can note that the amount of Ca has decreased which is due to dissolution of limestone after reaction with the acidic fluoride water which is confirmed by corresponding increase in the amount of Ca in the treated water [33]. The table also shows that the percentage weight of carbon has increased. Since both of the acids used in the experiment contains carbon and they precipitate as their respective salts increasing the percentage of carbon. In the limestone after use with AA (Fig. 5B), the observed appearance of the white grains can be attributed to formation of fluorite. The appearance of white colors at the edges of the particles in the SEM micrographs (Fig. 5C) of the limestone sample after use may be attributed to the calcium citrate crystals formed during the process. The amount of oxygen remains almost same probably due to the presence of the element in the crude limestone as well as in the acid. Although Mg and Si have been found in low amount in the unused limestone, in case of used limestone with AA the weight% and atomic% of these to atoms are quite high. This may be due to dissolution of calcium carbonate of the surface leaving Si and Mg to increase. Another possibility is that in the particular position where EDX has been taken, the percentage of these two elements is high. In the limestone used with CA the percentage of these two elements are lower than that in the crude limestone. This can be attributed to precipitation of the calcium citrate salt on the surface of the limestone particles suppressing the percentage of Si and Mg on the surface. Thus the SEM and EDX data obtained from the experiments reveals that fluoride has been precipitated as well as adsorbed on the surface of the limestone.

Table 2
The characteristic X-ray values emitted from the elements present in limestone on interaction of the primary electron beam and the weight cum atomic percentage of the elements before and after use of limestone with CA.

Element	Shell	X-ray energy (keV)	Weight% (before)	Atomic% (before)	Weight% (after use with AA)	Atomic% (after use with AA)	Weight% (after use with CA)	Atomic% (after use with CA)
Ca	Kα	3.6905	31.01	14.66	11.63	5.10	18.45	7.68
	Lα	0.3413						
C	Kα	0.2774	12.57	19.84	14.10	20.65	24.01	33.36
O	Kα	0.5249	53.64	63.53	51.49	56.63	54.33	56.67
F	Kα	0.6768	0	0	10.60	9.81	1.21	1.06
Mg	Kα	1.2536	0.96	0.75	1.78	1.29	0.39	0.27
Si	Kα	1.7398	1.82	1.23	10.41	6.52	1.61	0.96

2.7. XPS study

The XPS spectra of the limestone samples before and after use with AA and CA have been reported in our previous paper [33]. Considerable intensities corresponding to F-1S electron binding energy (BE) were observed in the fluorine XPS of the surface of limestone recorded after use with both AA (BE = 684.201 eV) and CA (BE = 685.625 eV) whereas there was no intensity corresponding to fluorine in the limestone sample before use [50,51]. This indicates that fluoride is either precipitated as CaF_2 or adsorbed on the surface of the limestone. On the other hand, in the carbon XPS, the observed relative areas (%) of the intensity peaks corresponding to C-1s BE of 284.6, 286.4 and 289.3 eV were 68.4:12.0:19.6, 52.7:18.8:28.5 and 41.2:27.1:31.7 for limestone samples before use, after use with AA and after use with CA, respectively. The increase in the relative intensities at 286.4 and 289.3 eV after use can be attributed to carbons of acetate and citrate ions [33]. Since acid was added to the water before filtration through limestone column and salts of respective acids has been precipitated as evident from the X-ray, IR, TGA-DSC and SEM-EDX analysis, there is a chance of increasing carbon adsorption on the surface of the limestone [52]. Thus, the XPS results are in agreement with the information obtained from other analytical tools described in the previous sections that in addition to adsorption of fluoride, adsorption of acetate and citrate ions also takes place on the surface of the limestone during the process.

3. Conclusion

The following conclusions can be drawn from the present study:

- During the limestone defluoridation in presence of AA or CA, the acids degrade limestone to Ca-salts of the acids.
- There is a greater morphological effect of AA than that of CA on the limestone. The lesser morphological change of the limestone when used with CA than with AA is due to inhibition of limestone degradation by precipitates of calcium citrate.
- Some fluorites are formed due to adsorption of fluoride on limestone or due to penetration by fluoride slightly into the limestone near the surfaces.
- There is no significant change in the limestone morphology of the limestone excluding the deposited precipitates after use in for the defluoridation.
- Therefore the used limestone remains fit for reuse in the fluoride removal process after removing the precipitates. The used limestone should also retain its quality required for its normal use in cement manufacturing.

4. Experimental

4.1. Materials

Crude limestone was obtained from Bokajan Cement Factory, a government of India enterprise at Bokajan, Assam, India. The limestone was crushed and segregated into different particle sizes, *viz.*, 2–3 mm and 3–4 mm for the fluoride removal column experiments. AR grade glacial acetic acid (AA), citric acid (CA) and NaF, for the preparation of acidic fluoride solutions were obtained from Merck, Mumbai were used as such.

4.2. Methods

A column of length 44 cm and diameter 4 cm was filled with crushed limestone particles of 2–3 mm size to which 10 mg/L F^- solution containing 0.10 M AA, was added to fill up the vacant space up to the top level of limestone column. The pH of the water at this AA and CA concentrations were 2.87 and 2.09, respectively. The total volume of water in such a crushed limestone column was about 200 mL. In this experiment the columns were charged with water once in a day and discharged in two or three parts, after 6, 12 and 24 h and then recharged instead of a continuous flow column test with fixed flow rates. The defluoridation process with charging and discharging every day was continued for several days (up to 30 days) using the same limestone column. The F^- concentration and final pH of the water withdrawn after 6, 12 and 24 h were measured. The limestone continuously used for 30 days was taken for the morphological study as used limestone. The experiment was repeated with same concentrations of CA in place of AA maintaining other conditions same, to observe the effect of CA in this fluoride removal process. Limestone samples were collected from different height of the column and dried in oven at 120 °C for 3 h to evaporate the water.

4.3. Equipment

XRD and IR were recorded on a Rigaku X-ray diffractometer, Miniflex UK and a Nicolet FTIR Spectrophotometer, respectively. Thermal analysis was done on a Shimadzu thermogravimetric analyzer TGA 50 and a Shimadzu DSC 60. Limestone surface analysis before and after the treatment was performed on KRATOS ESCA model AXIS 165 with accuracy <0.3 eV. SEM micrographs were taken on a scanning electron microscope, make JEOL model JSM-6390LV. Concentrations of F^- were measured on an Orion Multiparameter Kit ion meter using an Orion ion selective electrode for fluoride. Total ionic strength adjustment buffer (TISAB-III) was used to control ionic strength and de-complex fluoride. The pH was measured on a Systronics μ-pH System. Calcium was determined by using Perkin Elmer AA200 atomic absorption spectrophotometer.

Acknowledgements

The authors gratefully thank the Department of Science and Technology, New Delhi, India for financial support under the projects DST/TDT/WTI/2k7/24 and DST/TSG/WP/2007/14. The authors also thank Bokajan Cement Factory, Bokajan, Assam, India for gift samples of limestone.

References

[1] S. Meenakshi, R.C. Maheswari, J. Hazard. Mater. 137 (2006) 456–563.
[2] S. Ayoob, A.K. Gupta, Crit. Rev. Environ. Sci. Technol. 36 (2006) 433–487.
[3] A.K. Susheela, A Treatise on Fluorosis, Fluorosis Research & Rural Development Foundation, Delhi, 2001.
[4] Bureau of Indian Standards (BIS), Indian Standard Specification for Drinking Water, IS 10500, 1991, pp. 2–4.
[5] World Health Organization (WHO), Guideline for Drinking Water Quality, third ed., 2008, pp. 375–377.
[6] A.M. Raichur, M.J. Basu, Sep. Purif. Technol. 24 (2001) 121–127.
[7] D. Thakre, S. Jagtap, A. Bansiwal, N. Labhsetwar, S. Rayalu, J. Fluor. Chem. 131 (2010) 373–377.
[8] M. Karthikeyan, K.K. Satheesh Kumar, K.P. Elango, J. Fluor. Chem. 130 (2009) 894–901.
[9] J.L. Davila-Rodriguez, V.A. Escobar-Barrios, K. Shirai, J.R. Rangel-Mendez, J. Fluor. Chem. 130 (2009) 718–726.
[10] S. Saha, Water Res. 27 (1993) 1347–1350.
[11] E.J. Reardon, Y. Wang, Environ. Sci. Technol. 34 (2000) 3247–3253.
[12] G. Singh, B. Kumar, P.K. Sen, J. Majumdar, Water Environ. Res. 71 (1999) 36–42.
[13] Z. Amer, B. Bariou, N. Mameri, M. Taky, S. Nicolas, A. Elmidaoui, Desalination 133 (2001) 215–223.
[14] A. Dieye, C. Larchet, B. Auclair, C. Mar-Diop, Eur. Polym. J. 34 (1998) 67–75.
[15] N. Mameri, H. Lounici, D. Belhocine, H. Grib, D.L. Piron, Y. Yahiat, Sep. Purif. Technol. 24 (2001) 113–119.
[16] M. Hichour, F. Persin, J. Sandeaux, J. Molenat, C. Gavach, Rev. Sci. Eau. 12 (1999) 671–686.
[17] M. Hichour, F. Persin, J. Sandeaux, C. Gavach, Sep. Purif. Technol. 18 (2000) 1–11.
[18] S.K. Adhikari, U.K. Tipnis, W.P. Harkare, K.P. Govindan, Desalination 71 (1989) 301–312.
[19] M.A. Menkouchi Sahli, S. Annouar, M. Tahaikt, M. Mountadar, A. Soufiane, A. Elmidaoui, Desalination 212 (2007) 37–45.
[20] M. Sarkar, A. Banerjee, P.P. Pramanick, A.R. Sarkar, Chem. Eng. J. 131 (2007) 329–335.
[21] W. Nigussie, F. Zewge, B.S. Chandravanshi, J. Hazard. Mater. 147 (2007) 954–963.
[22] G. Karthikeyan, S.S. Ilango, Iran. J. Environ. Health Sci. Eng. 4 (2007) 21–28.
[23] G.S. Chauhan, R. Kumar, M. Verma, J. Appl. Polym. Sci. 106 (2007) 1924–1931.
[24] S.S. Tripathy, J. Bersillon, K. Gopal, Sep. Purif. Technol. 50 (2006) 310–317.
[25] B.D. Turner, P.J. Binning, S.L.S. Stipp, Environ. Sci. Technol. 39 (2005) 9561–9568.
[26] B.D. Turner, P.J. Binning, S.W. Sloan, J. Contam. Hydrol. 95 (2008) 110–120.
[27] M. Yang, T. Hashimoto, N. Hoshi, H. Myog, Water Res. 33 (1999) 3395–3402.
[28] S. Vigneswaran, C. Visvanathan, Water Treatment Processes: Simple Options, CRC Press, Boca Raton, FL, 1995.
[29] W. Augustyn, M. Dzieqielewska, A. Kossuth, Z. Librant, J. Fluor. Chem. 12 (1978) 281–292.
[30] D.K. Nordstorm, E.A. Jenne, Geochim. Cosmochim. Acta 41 (1977) 175–188.
[31] T. Majima, H. Takatsuki, Water Purif. Liquid Wastes Treat. 28 (1987) 433–443.
[32] S.K. Nath, R.K. Dutta, Indian J. Chem. Technol. 17 (2010) 120–125.
[33] S.K. Nath, R.K. Dutta, Clean-Soil Air Water 38 (2010) 614–622.
[34] S. Gunasekaran, G. Anbalagan, S. Pandi, J. Raman Spectrosc. 37 (2006) 892–899.
[35] E.D. Glover, R.F. Sippel, Am. Mineral. 47 (1962) 1156–1165.
[36] D. Simonsson, Ind. Eng. Chem. Process Des. Dev. 18 (1979) 288–292.
[37] I.C. Zamba, M.G. Stamatakis, F.A. Cooper, P.G. Themelis, C.G. Zambas, Mater. Charact. 58 (2007) 1229–1239.
[38] C. Cardell, D. Benavente, J. Rodríguez-Gordillo, Mater. Charact. 59 (2008) 1371–1385.
[39] S. Mukherjee, S.K. Srivastava, Energy Fuels 20 (2006) 1089–1096.
[40] Mineral Powder Diffraction File Data Book, No. 5-586, ICDD, 1993.
[41] R. Aldaco, A. Garea, A. Irabien, Ind. Eng. Chem. Res. 45 (2006) 796–802.
[42] A.W. Musumeci, R.L. Frost, E.R. Waclawik, Spectrochim. Acta Part A 67 (2007) 649–661.
[43] C.N.R. Rao, Chemical Applications of IR Spectroscopy, Academic Press, London, 1963, p. 23.
[44] K. Nakamoto, Infrared and Raman Spectra of Coordination Compounds, Part B, fifth ed., Wiley Inter Science, 1997.
[45] M. Nara, H. Torii, M. Tasumi, J. Phys. Chem. 100 (1996) 19812–19817.
[46] D.L. Pavia, G.M. Lampman, G.S. Kriz, J.R. Vyvyan, Introduction to Spectroscopy, forth ed., Brooks/Cole, Cengage, Learning, Bellingham, WA, 2009.
[47] Digitalfire Ceramic Materials Database, http://www.digitalfire.com.
[48] F.W. Fifield, P.J. Haines, Environmental Analytical Chemistry, second ed., Blackwell Science, Oxford, United Kingdom, 2000.
[49] B. Singh, N.P. Singh, J. Therm. Anal. Calorim. 89 (2007) 159–162.
[50] S. Chander, D.W. Fuerstenau, Colloids Surf. 13 (1985) 137–144.
[51] Y. Kawamoto, K. Ogura, M. Shojiya, M. Takahashi, K. Kadono, J. Fluor. Chem. 96 (1999) 135–139.
[52] N. Suzuki, X-ray Photoelectron Spectroscopy and its Application to Carbon, Carbon Alloys, Elsevier Science Ltd., 2003, pp. 211–222.